Journal of Sound and Vibration (1997) **207**(1), 95–121

ACTIVE ISOLATION OF STRUCTURAL VIBRATION ON A MULTIPLE-DEGREE-OF-FREEDOM SYSTEM, PART II: EFFECTIVENESS OF ACTIVE CONTROL STRATEGIES

P. Gardonio, S. J. Elliott and R. J. Pinnington

Institute of Sound and Vibration Research, University of Southampton, Southampton SO17 1BJ, England

(*Received* 8 *July* 1996, *and in final form* 19 *June* 1997)

This is the second of two companion papers concerned with the active control of structural vibration transmission. Five different active control strategies have been studied for the reduction of structural power transmission from a source to a receiver via a number of active mounts. The effects of transducer errors and the problems created by the presence of an uncontrolled flanking excitation acting on the receiver have been analyzed. Minimization of the total power transmitted to the receiver through the mounts has been compared with more practical control strategies at the junctions connecting the mounts to the plate: the cancellation of out-of-plane velocities, the cancellation of out-of-plane forces, the cancellation of the power due only to the out-of-plane velocities and forces and the minimization of the sum of squared out-of-plane velocities and weighted square forces. The control of total power gives the best results under ideal conditions but, for realistic cases, characterized by measurement errors and flanking paths, the cancellation of velocity or force is more effective than the active control of measured power. The minimization of the sum of squared velocities and weighted squared forces gives a particularly interesting result since the performance of the active control system is then almost the same as that of minimizing total power and this performance is not sensitive to measurement errors or flanking paths.

1. INTRODUCTION

In recent years, an increasing amount of work has been published on active control of vibration transmission. The first examples of commercial active mounts have appeared and the main applications have thus far been automotive suspension [1], seismic isolation of experimental platforms and precision manufacturing machines [2] and the isolation of machines [3]. With reference to the last category of applications, there are several examples of systems in which active isolators are used successfully. Car, ship, helicopter and aeroplane engines transmit high levels of vibration to the structure of the vehicle on which they are mounted and this vibration can cause structural failure or unwanted noise. Electrical motors in domestic machines (washing machines, refrigerators and air conditioning systems) also generate vibration that is transmitted to the machine case, which then generates noise.

This paper presents a theoretical study of the active isolation of vibration transmission to a structure on which a machine is mounted. In the companion paper [4] the details of the matrix model formulation and the passive dynamic behaviour of the system were

0022–460X/97/410095 + 27 $25.00/0/sv971153

introduced, while in this paper the effectiveness of different active control strategies is examined.

The performance of traditional passive mounts is limited by the simultaneous need for a stiff mount to provide a reaction to the static load of the source and the need for a soft mount to limit the vibration transmission due to the dynamic excitation of the source [1–3, 5–7]. The damping supplied by a mount reduces the vibration transmission at its resonance frequency but compromises the isolation at higher frequencies [1, 5, 6].

The use of an active control system can overcome these limitations and allows higher levels of vibration isolation. The secondary actuator can be placed inside the mount or can be applied separately to the receiver by using an actuator in series with a seismic mass or by using a piezoceramic actuator attached to the receiver [8, 9]. When the actuator is mounted inside the suspension system, two different configurations are possible: in series or in parallel with the passive member of the suspension. In this paper, the actuator is assumed to be in parallel with the passive mount and to provide only an axial excitation.

Most of the studies of active isolation refer to simple one-degree-of-freedom models that do not accurately represent many of the phenomena that occur in practice. von Flotow [10] has discussed the dynamics of the different parts of an isolator in detail. He pointed out that both the source and the receiver are distributed systems, the dynamics of which can only be modelled as rigid bodies at low excitation frequencies. In a mid-frequency band between the fundamental resonance and the region of high modal overlap these systems can be modelled as modal systems. At higher frequencies, a reasonable approach is to model these systems as equivalent infinite structures in which only propagating phenomena occur. In many situations, the machine is much stiffer than the receiver, and the mid- and high-frequency regions referred to above are moved up in frequency. The mount dynamics are characterized by low frequency resonances due to the mass vibrating on the elastic mount while, at higher frequencies, the resonances due to the modal behaviour of the distributed mount must be considered. Blackwood *et al*. [3] and Jenkins *et al*. [11] provided preliminary studies of active isolation control by considering the effects induced by a distributed receiver and by a multi-mount suspension system. This paper presents a detailed theoretical study of an active isolator by modelling multi-distributed mounts and by considering a distributed receiver. It is assumed that the source structure has a fundamental resonance at a frequency above the range examined and so it can be modelled simply as a rigid body. A generalized external force is used to represent the source excitation, which is usually due to impacts, imbalanced rotation of oscillating members and bearing and gear meshing vibration [12]. In particular, a case has been studied in which the source is a rigid mass free to move in two directions and rotate in a plane, connected to an infinite or finite plate by a pair of active mounts. A detailed study of the passive vibration transmission of such system has been provided in the companion paper [4].

Pan *et al*. [13] studied the dynamics of an active isolator by considering power transmission and thus extended the modelling of passive isolation systems in terms of power [14, 15] to the modelling of active isolators. As is shown in the companion paper [4], the dynamics of a multi-mount isolator, having distributed members with multi-directional vibration, is quite complicated but by considering power transmission almost all of the important information is retained. Power is not only considered simply as a good parameter for describing the vibration, but also many authors [16–21] have started to consider power minimization as an objective for the active control architecture in structural isolation. Pan *et al*. [22, 23] applied this new strategy to isolator systems and showed that it is possible to reduce the power transmission to a receiver.

The minimization of total power transmission must by definition be the optimal strategy. However, the difficulty in measuring such a parameter and the effects produced by flanking paths make this control approach difficult to carry out in practice.

Therefore, the effectiveness of alternative control strategies has been studied and gauged with reference to the minimization of total power, which has been used as a "benchmark" for active isolation of structural vibration transmission. Four alternative control strategies have been considered: the conventional strategies of cancelling velocities or forces at the receiver junctions, the minimization of an estimate of power (power due to out-of-plane velocities and forces measured at the receiver junctions) and, finally, the minimization of the sum of squared out-of-plane velocities and weighted squared out-of-plane forces at the receiver junctions. These control strategies require relatively simple measuring devices and this is a key simplification in making these approaches practical.

The performance of each of these control strategies is first estimated under ideal conditions and then in the presence of an uncontrolled flanking path acting on the receiver, or in the presence of measurement errors which are always produced by the sensors. Scheuren *et al*. [24] have presented some experimental results on the effects of a flanking source when the active isolation is based on a conventional cost function. In this paper, these effects are also considered for an uncontrolled flanking excitation when the power cost function is utilized.

2. CONTROL STRATEGIES

The isolating system studied consisted of a rigid mass acting as a source, connected to a receiver plate through a pair of mounts, each of which has an internal secondary actuator which can generate an axial control force. A sketch of such a system is shown in Figure 1. A detailed description of the matrix model used to describe its dynamics was formulated and presented in the companion paper [4]. The velocities and forces at the source and receiver junctions are grouped respectively into two vectors $\mathbf{v}_{sr}$ and $\mathbf{f}_{sr}$ and two equations were used to relate these parameters to the primary-flanking $\mathbf{q}_{pf}$ and control $\mathbf{q}_s$ excitation vectors [4],

$$\mathbf{v}_{sr} = \mathbf{Q}_{pv}\mathbf{q}_{pf} + \mathbf{Q}_{sv}\mathbf{q}_s, \qquad \mathbf{f}_{sr} = \mathbf{Q}_{pf}\mathbf{q}_{pf} + \mathbf{Q}_{sf}\mathbf{q}_s, \tag{1, 2}$$

where the four matrices $\mathbf{Q}_{pv}$, $\mathbf{Q}_{sv}$, $\mathbf{Q}_{pf}$ and $\mathbf{Q}_{sf}$ can be derived by using equations (22–25) of reference [4].

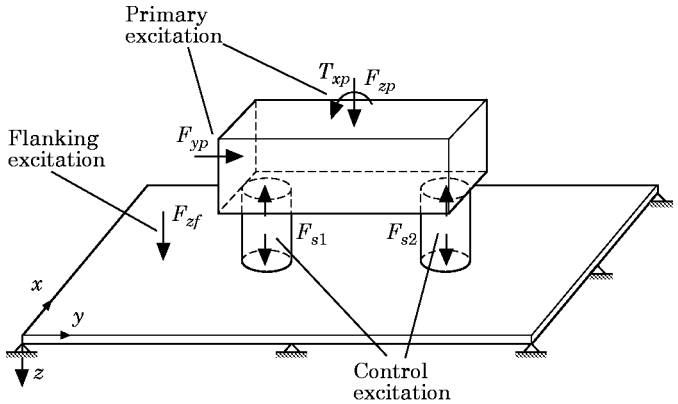

Figure 1. The active isolation system.

The strategies considered here for active control can all be expressed in terms of a quadratic cost function which is minimized and this can always be written in the form [25–27]

$$J = \mathbf{q}_s^{\mathrm{H}} \mathbf{A} \mathbf{q}_s + \mathbf{q}_s^{\mathrm{H}} \mathbf{b} + \mathbf{b}^{\mathrm{H}} \mathbf{q}_s + c. \tag{3}$$

The control source that minimizes this quadratic equation is given by [25–27]

$$\mathbf{q}_s(opt) = -\mathbf{A}^{-1}\mathbf{b}. \tag{4}$$

The control strategy of (a) *minimizing total power transmitted by the source to the receiver* (J_p) [22, 23] was compared with two conventional strategies that are (b) the *cancellation of axial input velocities to the receiver* (J_v) [3, 12] and (c) the *cancellation of axial input forces to the receiver* (J_f) [3] and also compared with two alternative cost functions based on (d) the *minimization of an estimate of power transmitted by the source to the receiver* (J_a) given by the product of the out-of-plane velocities and forces at the receiver junctions and (e) the *minimization of the sum of squared out-of-plane input velocities and the weighted squared out-of-plane input forces to the receiver* ($J_{v,f}$). In this paper these five control strategies will be referred to as (*a*) *total power minimisation*, (b) *velocity cancellation*, (c) *force cancellation*, (d) *axial power minimization* and (e) *velocity and force minimization*.

When the total power is minimized, the cost function is

$$J_p = \tfrac{1}{2}\mathrm{Re}\,(\mathbf{f}_r^{\mathrm{H}} \mathbf{v}_r) = \tfrac{1}{4}(\mathbf{f}_r^{\mathrm{H}} \mathbf{v}_r + \mathbf{v}_r^{\mathrm{H}} \mathbf{f}_r), \tag{5}$$

where all six velocities and forces at each of the receiver junctions are given by the following two equations

$$\mathbf{v}_r = \mathbf{R}_p \mathbf{v}_{sr}, \qquad \mathbf{f}_r = \mathbf{R}_p \mathbf{f}_{sr}, \tag{6, 7}$$

in which $\mathbf{R}_p = [\mathbf{0}_{t\times t}\, \mathbf{I}_{t\times t}]$ and $\mathbf{0}_{t\times t}$ and $\mathbf{I}_{t\times t}$ are, respectively, a zero matrix and a unit matrix and t is the dimension of the source and receiver vectors. The two matrices in the quadratic form of equation (3) are then given by

$$\mathbf{A}_p = \tfrac{1}{4}(\mathbf{Q}_{sf}^{\mathrm{H}} \mathbf{R}_p^{\mathrm{T}} \mathbf{R}_p \mathbf{Q}_{sv} + \mathbf{Q}_{sv}^{\mathrm{H}} \mathbf{R}_p^{\mathrm{T}} \mathbf{R}_p \mathbf{Q}_{sf}),$$

$$\mathbf{b}_p = \tfrac{1}{4}(\mathbf{Q}_{sf}^{\mathrm{H}} \mathbf{R}_p^{\mathrm{T}} \mathbf{R}_p \mathbf{Q}_{pv} \mathbf{q}_{pf} + \mathbf{Q}_{sv}^{\mathrm{H}} \mathbf{R}_p^{\mathrm{T}} \mathbf{R}_p \mathbf{Q}_{pf} \mathbf{q}_{pf}). \tag{8, 9}$$

When axial velocity cancellation is implemented then the cost function has the form

$$J_v = \bar{\mathbf{v}}_r^{\mathrm{H}} \bar{\mathbf{v}}_r \tag{10}$$

and $\bar{\mathbf{v}}_r = \{\dot{w}_{r1}\ \dot{w}_{r2}\}^{\mathrm{T}}$ is a vector containing only the out-of-plane velocities at the receiver junctions. This vector can be derived by using equation (6), but the matrix $\mathbf{R}_p$ is replaced by a matrix $\mathbf{R}_v = [\mathbf{0}_{2\times t}\, \mathbf{H}_{2\times t}]$: matrix $\mathbf{H}_{2\times t}$ contains unitary values that correspond to the out-of-plane degrees of freedom. The two matrices in equation (3) are then given by

$$\mathbf{A}_v = \mathbf{Q}_{sv}^{\mathrm{H}} \mathbf{R}_v^{\mathrm{T}} \mathbf{R}_v \mathbf{Q}_{sv}, \qquad \mathbf{b}_v = \mathbf{Q}_{sv}^{\mathrm{H}} \mathbf{R}_v^{\mathrm{T}} \mathbf{R}_v \mathbf{Q}_{pv} \mathbf{q}_{pf}. \tag{11, 12}$$

When axial force cancellation is implemented then the cost function has the form:

$$J_f = \bar{\mathbf{f}}_r^{\mathrm{H}} \bar{\mathbf{f}}_r, \tag{13}$$

where $\bar{\mathbf{f}}_r = \{N_{zr1}\ N_{zr2}\}^{\mathrm{T}}$ is a vector containing the out-of-plane forces at the receiver junctions. This vector can be derived by using equation (7) but the matrix $\mathbf{R}_p$ is replaced by a matrix $\mathbf{R}_f = [\mathbf{0}_{2\times t}\, \mathbf{H}_{2\times t}]$. The two matrices in equation (3) are then given by

$$\mathbf{A}_f = \mathbf{Q}_{sf}^{\mathrm{H}} \mathbf{R}_f^{\mathrm{T}} \mathbf{R}_f \mathbf{Q}_{sf}, \qquad \mathbf{b}_f = \mathbf{Q}_{sf}^{\mathrm{H}} \mathbf{R}_f^{\mathrm{T}} \mathbf{R}_f \mathbf{Q}_{pf} \mathbf{q}_{pf}. \tag{14, 15}$$

If axial power is minimized the cost function assumes exactly the same form as equation (5) but only the velocity and force vectors containing the out-of-plane parameters $(\bar{\mathbf{v}}_r, \bar{\mathbf{f}}_r)$ are considered:

$$J_a = \tfrac{1}{2}\mathrm{Re}\,(\bar{\mathbf{f}}_r^{\mathrm{H}}\bar{\mathbf{v}}_r) = \tfrac{1}{4}(\bar{\mathbf{f}}_r^{\mathrm{H}}\bar{\mathbf{v}}_r + \bar{\mathbf{v}}_r^{\mathrm{H}}\bar{\mathbf{f}}_r). \tag{16}$$

The two matrices in equation (3) are then given by

$$\mathbf{A}_a = \tfrac{1}{4}(\mathbf{Q}_{sf}^{\mathrm{H}}\mathbf{R}_f^{\mathrm{T}}\mathbf{R}_v\mathbf{Q}_{sv} + \mathbf{Q}_{sv}^{\mathrm{H}}\mathbf{R}_v^{\mathrm{T}}\mathbf{R}_v\mathbf{Q}_{sf}), \qquad \mathbf{b}_a = \tfrac{1}{4}(\mathbf{Q}_{sf}^{\mathrm{H}}\mathbf{R}_f^{\mathrm{T}}\mathbf{R}_v\mathbf{Q}_{pv}\mathbf{q}_{pf} + \mathbf{Q}_{sv}^{\mathrm{H}}\mathbf{R}_v^{\mathrm{T}}\mathbf{R}_f\mathbf{Q}_{pf}\mathbf{q}_{pf}). \tag{17, 18}$$

Finally, if a cost function which considers both velocities and forces are considered is minimized, then both the velocity and force vectors containing the out-of-plane parameters $(\bar{\mathbf{v}}_r, \bar{\mathbf{f}}_r)$ must be used. Such a cost function is given by

$$J_{v,f} = \bar{\mathbf{v}}_r^{\mathrm{H}}\bar{\mathbf{v}}_r + \mu\bar{\mathbf{f}}_r^{\mathrm{H}}\bar{\mathbf{f}}_r, \tag{19}$$

where μ is a weighting factor which is used to combine the two parameters in the cost function. The weighting factor μ has the dimensions of mobility squared (s/kg). In the simulations reported here, μ was set equal to the square of the point mobility of an infinite receiving plate of an appropriate thickness and was thus independent of frequency. It was found, however, that the exact value of this parameter did not significantly affect the results. The two matrices in equation (3) are then given by

$$\mathbf{A}_{v,f} = \mathbf{Q}_{sv}^{\mathrm{H}}\mathbf{R}_v^{\mathrm{T}}\mathbf{R}_v\mathbf{Q}_{sv} + \mu\mathbf{Q}_{sf}^{\mathrm{H}}\mathbf{R}_f^{\mathrm{T}}\mathbf{R}_f\mathbf{Q}_{sf}, \qquad \mathbf{b}_{v,f} = \mathbf{Q}_{sv}^{\mathrm{H}}\mathbf{R}_v^{\mathrm{T}}\mathbf{R}_v\mathbf{Q}_{pv}\mathbf{q}_{pf} + \mu\mathbf{Q}_{sf}^{\mathrm{H}}\mathbf{R}_f^{\mathrm{T}}\mathbf{R}_f\mathbf{Q}_{pf}\mathbf{q}_{pf}. \tag{20, 21}$$

Total power minimization must by definition be the optimal control strategy. It acts as a benchmark against which the other four control strategies can be judged. The total power is a cost function that allows the simultaneous weighting of different types of parameters. In particular, it is possible to weight simultaneously the effects of linear and angular velocities and the effects of forces and moments. The conventional strategies of cancelling the axial velocities or forces are limited in this sense since linear or angular parameters can be considered only in isolation. The two alternative cost functions based on axial power minimization and velocity and force minimization also use only out-of-plane velocity and force parameters at the receiver junctions.

3. ACTIVE CONTROL EFFECTIVENESS

In this section the performance of an active isolating system is examined by considering the five control strategies when a "combined primary excitation" perturbs the source. The combined primary excitation consists of axial ($\mathbf{F}_{zp}$) and transverse ($\mathbf{F}_{yp}$) unit forces and a unit torque ($\mathbf{T}_{xp}$). These excitations are harmonic with time dependence of the form $\exp(\mathrm{j}\omega t)$. In all of the simulations conducted this form of primary excitation was used, applied to the system shown in Figure 1, the dimensions and physical characteristics of which are the same as those assumed in the companion paper [4]. The simulations were limited to a frequency range between 0 and 1000 Hz and the performance of the active control isolation was studied by considering the total power input into the receiver before and after control.

3.1. INFINITE RECEIVER PLATE

The physical effects generated by the active control are introduced here by considering the total power minimization control strategy when the receiver is a 100 mm thick infinite

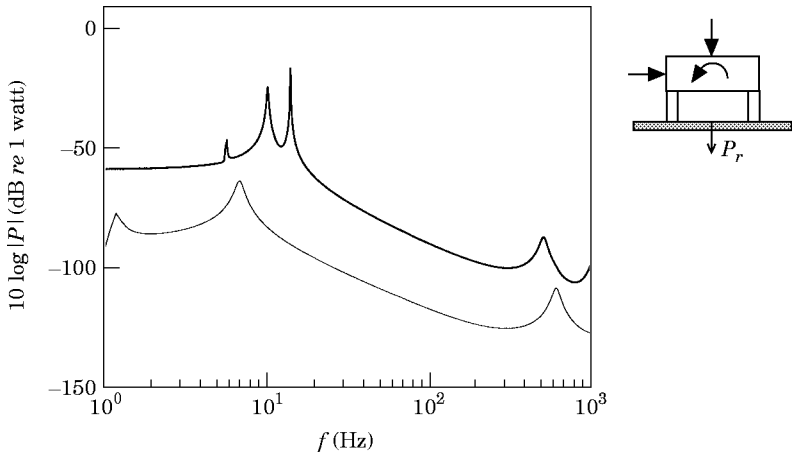

Figure 2. The power transmitted to an infinite 100 mm thick plate when a combined excitation acts on the source. ——, Uncontrolled system; ———, total power minimization.

plate. The frequency distribution of the power transmission to the receiver can be more easily understood when the receiver is an infinite plate, since the peaks associated with the normal modes of a finite plate do not exist. Also thick plate was chosen to reduce the dissipative effects of the infinite receiver at low frequencies and so the peaks related to the three rigid modes of the isolator (axial mode, transverse mode and pitching mode) are quite distinct and can be easily identified in the frequency band between 6 and 12 Hz [4].

In Figure 2 is shown the power transmitted to the receiver without control, and when total power is minimized for a range of single frequency excitation. An average attenuation of about 25 dB is obtained over the frequency range examined, with an attenuation of about 80 dB at rigid body resonance at about 12 Hz. The response of the system after control is now characterized by different resonance conditions, and at these resonance frequencies the attenuation of power transmission is limited to about 10 dB.

When active control is implemented, only two of the three rigid body modes are present, and they have resonance frequencies different from those of the passive system [4]. The isolator resonance at 500 Hz due to longitudinal waves in the mounts is also cancelled and a new peak at around 600 Hz is introduced which is due to a flexural wave resonance in the mounts [4]. All of these changes to the system's response are related to the fact that, when total power is minimized, the axial forces at the mount ends are greatly attenuated by the action of the control forces. The axial control forces completely decouple the axial oscillation of the source from the mounts, and the axial rigid body mode of the source and the axial mode due to the longitudinal waves propagating in the mounts disappear. The transverse and pitching modes are still present but are now controlled solely by the bending stiffness of the mounts (instead of bending and normal stiffness) and therefore their natural frequencies are reduced. In the companion paper [4] it was found that the natural frequencies of the transverse and pitching modes were approximately given by considering respectively the transverse stiffness (k_t) and the mass (m) of the source and by considering the pitching stiffness (k_p) and the moment of inertia of the mass (I_G). The same approach can be used to determine the natural frequencies after control but, because the transverse and pitching modes after control are now controlled by the mounts acting as springs reacting only to rotation, both the transverse and pitching stiffnesses of the

mounts are changed and assume the following values: $k_t' = k_p' = 6EI_x/h^2$ [5]. Therefore, the new natural frequencies are

$$f_t' = (1/2\pi)\sqrt{2k_t'/m} = 1{\cdot}31 \text{ Hz}, \qquad f_p' = (1/2\pi)\sqrt{2k_p'/I_G} = 7{\cdot}5 \text{ Hz}. \qquad (22, 23)$$

These two values are close to the resonance conditions visible in Figure 2. Because there is no substantial axial excitation of the mounts, the resonance due to standing longitudinal waves in the mount is also cancelled. The source excitation is redirected to rotation and the resonance due to flexural standing waves in the mount is now more effectively excited than before active control.

After having described the main effects of active control on the dynamics of the system with reference to a thick receiver plate, the power transmission to the receiving plate can now be considered for various control strategies when the plate is of a more realistic thickness.

In Figure 3 is shown the frequency distribution of the power transmitted to a 5 mm thick infinite receiver plate without control and by controlling the total power transmitted to the receiver. Because the receiver plate is thinner than the plate considered above, the dissipative effect due to out-of-plane excitation is particularly high and the rigid mode resonances of the system without control are grouped together in a single broad peak at around 7 Hz. The average reduction in the power transmitted to the receiver is about 30 dB and the maximum and minimum reductions are about 45 dB and 6 dB, respectively. When active control is implemented, the dynamics of the system change in much the same way as seen in Figure 2. This is because the axial motion at the bottom of the mounts is greatly diminished and so the receiving structure appears to be almost rigid after control. The response of the system is characterized by two resonances related to the transverse and pitching modes of the isolator and the resonances due to flexural waves in the mounts replacing the resonances due to longitudinal waves. The two new rigid body resonances of the isolator are characterized by relatively sharp peaks. This is due to the fact that when there is no control excitation the transverse and the pitching modes are both characterized by axial, transverse and angular oscillations of the source [4]. The axial oscillation is controlled by the mount's axial stiffness and by the plate's out-of-plane reaction which is purely dissipative [4] and can thus induce a lot of damping into such modes. When the active control is implemented, the transverse and pitching modes are now controlled only

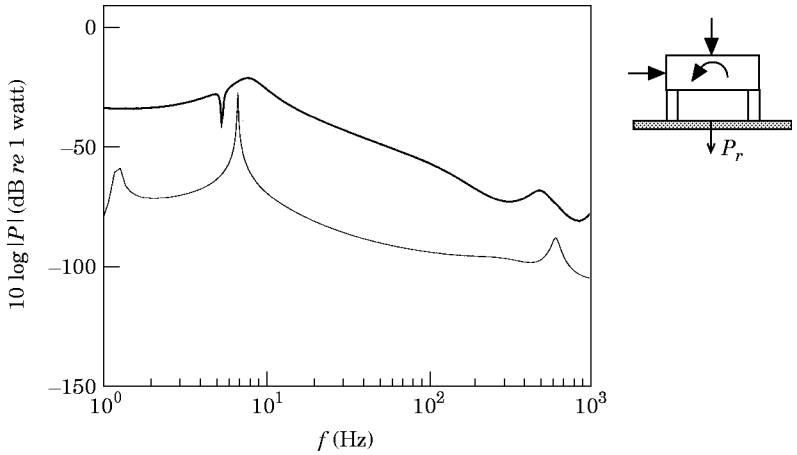

Figure 3. The power transmitted to an infinite 5 mm thick plate when a combined excitation acts on the source. ——, Uncontrolled system; – – –, total power minimization.

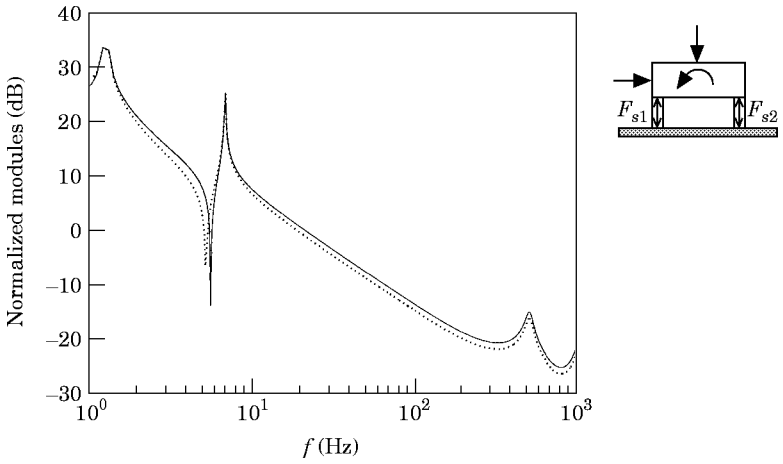

Figure 4. The modulus of the control sources for total power minimization strategy when the receiver is an infinite 5 mm thick plate. ——, Left mount; ....., right mount.

by the transverse and pitching oscillations of the source since the axial oscillation is completely uncoupled by the control forces. Moreover, the pitching oscillation is controlled by the mount's bending stiffness (instead of bending and normal stiffness) and therefore the natural frequencies of these two modes are related to transverse and bending stiffnesses of the mounts and with angular and in-plane reaction of the plate. The angular reaction of the plate is dissipative and reactive [4] and produces a relatively low damping effect; therefore, in the presence of the active control action the transverse and pitching modes of the isolator are more lightly damped than for the system without control.

In Figure 4 is shown the modulus of the control forces required by such a control strategy. Jenkins *et al*. [11] and Nelson *et al*. [28] studied the control force required to cancel the motion of the receiver for several different configurations of the control system using a single-degree-of-freedom model, of which the "parallel cancellation system" is the one most relevant here. The control force in this case was predicted to be relatively large at very low frequencies and to reduce as the frequency increases. This result suggests that the need for a soft mount, to monotonically reduce the natural frequency of the axial rigid body mode to be as low as possible, can be overcome, since the control force is not perturbed by the presence of such a resonance. By using a parallel cancellation system it should thus be possible to use a more rigid passive mount which produces better control over the static position of the source structure. The results presented in Figure 4 show the general trend predicted in references [11, 28], but also show a peak in the required force at the natural frequencies of the transverse and pitching modes. This suggests that increasing the stiffness of the mounts may generate some problems with a practical controller even when the parallel cancellation system is considered.

If the contribution to the power transmission due to each degree of freedom after control is calculated, it is found that the main contribution to the power transmission when the active control is implemented is due to the axial and transverse power at low frequency and to the angular power at high frequency. When the two rigid body modes of the controlled system are excited, the power transmission is due to all of the components. However, the axial power is larger than the total power transmitted to the receiver at these frequencies. The reason for this is that axial power is not transmitted to the receiver but is absorbed from the receiver. Power thus circulates in the system, with part of the transverse and angular power transmitted to the receiver being absorbed by the control

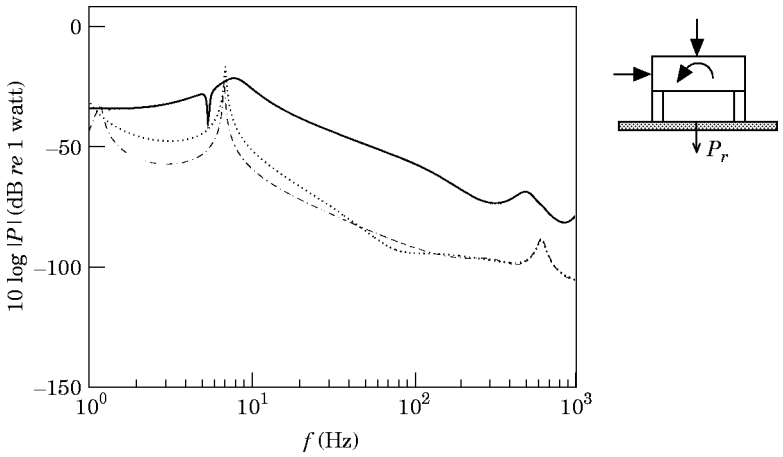

Figure 5. The power transmitted to an infinite 5 mm thick plate when a combined excitation acts on the source. ——, Uncontrolled system; –.–.–, velocity cancellation; ....., force cancellation.

sources as axial power. This behaviour is rather different from that shown in reference [4] for the passive isolator. When the active control of total power transmission is implemented, the transverse displacements and the rotations become as important as the axial displacements and a new phenomenon of "*power circulation*" characterizes the power transmission to the receiver.

The performance of the four active control strategies which use only axial velocity and force signals is shown in Figures 5 and 6. When these four control strategies are implemented in an infinite receiver plate, the dynamics of the system change in a similar way to that for total power minimization. The overall effects of these four control strategies are thus quite similar to each other in this case, and the average reduction in the power transmitted to the receiver is about 20 dB, while the maximum value is about 40 dB. However, when active control is implemented and the transverse or pitching rigid body modes of the isolator are excited, the performance is very poor, since the power transmitted to the receiver is even larger than before control. These alternative control approaches thus give good results at high frequency, where the attenuation is close to that obtained by

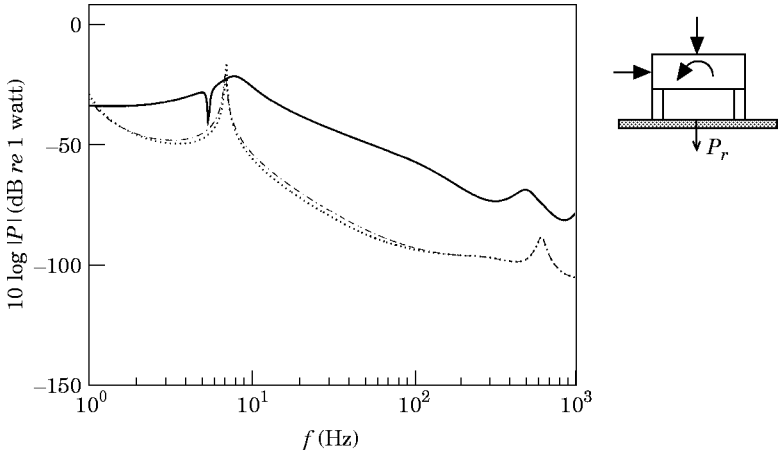

Figure 6. The power transmitted to an infinite 5 mm thick plate when a combined excitation acts on the source. ——, Uncontrolled system; –.–.–, velocity and force minimization; ....., axial power minimization.

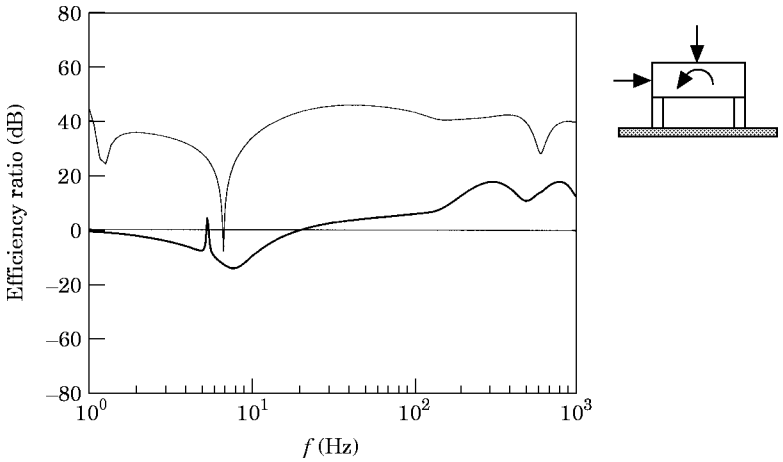

Figure 7. The efficiency of the passive isolation (——) and active isolation when velocity and force cost function is minimized (———) for an infinite 5 mm thick plate.

minimizing total power transmission. On the other hand, at low frequency these four control strategies produce poor results, particularly in the frequency band of the rigid body modes of the isolator.

The power transmission due to each degree of freedom after control has also been calculated. The velocity cancellation and force cancellation reduce the axial power transmission to zero and only transverse and angular power transmission occur. The transverse component of power is about 15 dB less than the angular power component. When the axial power is minimized, the residual angular power is the most important. The axial power is also negligible at high frequencies but in the frequency band of the rigid body modes it is quite large and is even larger than the total power transmitted in the frequency range between 0 and 100 Hz. This is due to the phenomenon of power circulation described above, and in this case the absorption of axial power from the receiver is so large that it is balanced by a quantity of angular power that is also higher than the total power transmitted to the receiver. As explained in Appendix A, when only some of the sources of power input to the receiver are accounted for in the cost function being minimized (in this case the control system is neglecting transverse and angular power input by the isolator), the power minimization control strategy will act to absorb power from only unobserved excitation. The power absorption could be so large that the total power transmission to the receiver is actually increased. When velocity and force control is used the transmission of power occurs mainly through angular power. A small amount of power is also transmitted by axial and transverse power. At low frequency, axial power transmission is greater than transverse power transmission while as the frequency rises this situation is reversed. It should be noted that in this control case there is a very little power circulation occurring between 9 and 70 Hz.

Jenkins *et al*. [11], Pan *et al*. [13] and Pan *et al*. [23] used the efficiency ratio [4, 28, 29] to represent the effectiveness of the passive and active isolation, which can be defined as the ratio of the power transmitted to the receiver by an isolator with rigid mounts and the power transmitted to the receiver by an isolator with flexible mounts:

$$E = P_t(\text{rigid mounts})/P_t(\text{passive or active mounts}). \tag{18}$$

In Figure 7 is shown the frequency distribution of the efficiency ratio when passive isolation and active control isolation based on velocity and force minimization are used. This

figure shows that the active isolator system on average increases the efficiency of the isolation by about 20 dB. The problems of passive isolation at low frequency, as discussed in the companion paper, are also overcome since, apart from the frequency at which the pitching rigid body mode is excited, the efficiency after active control is always larger than one.

3.2. FINITE RECEIVER PLATE

In this section the effects of active control are examined when the receiver is a finite plate of dimensions 1 m $\times$ 1·5 m $\times$ 5 mm. In Figure 8 is shown the frequency distribution of the power transmitted to the receiver without control and after minimization of the total power transmission. Although the power transmission before control is dominated by the resonances of the receiver structure, the results after control are quite similar to those for the isolator system mounted on an infinite receiver (see Figure 3). Total power control produces an average reduction of the power transmission of about 20 dB. The control of the rigid modes presents the same type of problems described in the previous section and the reduction of the power transmission is almost zero when the two rigid modes are excited by the controlled system. From 20 Hz to 200 Hz large attenuations are achieved, of the order of 30 dB, but for frequencies greater than 200 Hz the reduction is diminished to 20 dB. The reason for this reduction of the active control performance is related to the dynamics of the receiver. At around 80 Hz the flexural waves propagating in the receiver plate have wavelengths which are comparable to the distance between the two mounts, and so the coupling between the motion under the two mounts becomes weaker, and therefore the power injected by them becomes more independent [30]. Below about 200 Hz, where the flexural wavelength is long compared to the distance between the mounts, the axial secondary force generated by one mount can influence the moment introduced at the other mount [31] and thus the active mounts have a greater capability for controlling the total motion of the receiving structure.

The performance of the velocity and force cancellation control strategies is shown in Figure 9. At low frequencies the active isolator produces poor results, since the power transmitted to the receiver is of the same magnitude as the power transmitted by the passive isolator system when the transverse or pitching rigid body modes of the isolator are excited. The reason why the rigid body modes cannot be cancelled is due to the power circulation

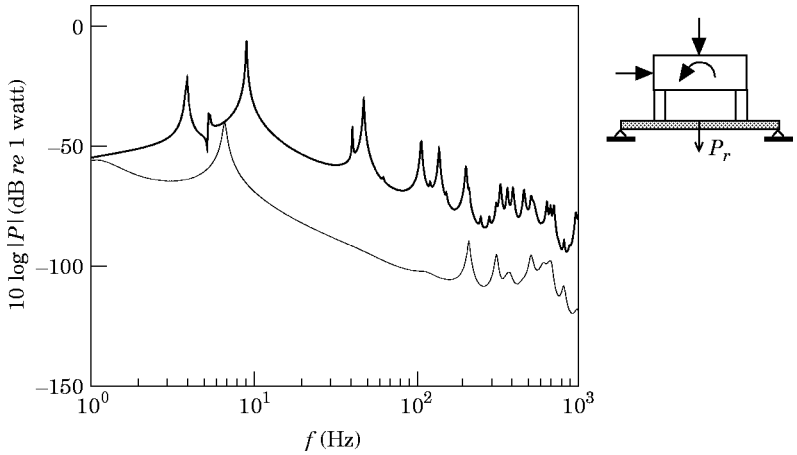

Figure 8. The power transmitted to a finite 5 mm thick plate when a combined excitation acts on the source. ——, Uncontrolled system; – – –, total power minimization.

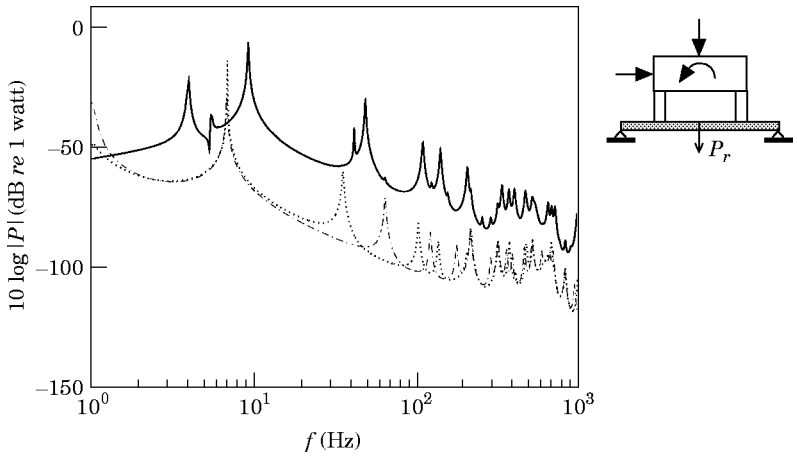

Figure 9. The power transmitted to a finite 5 mm thick plate when a combined excitation acts on the source. ——, Uncontrolled system; -·-·-, velocity cancellation, ..., force cancellation.

phenomenon described in the previous section. At frequencies above the two resonances of the rigid body modes and below 200 Hz, the control effectiveness of these two strategies is about the same as that of controlling total power. The power reduction becomes smaller when the modes of the distributed mounts and receiver plate are excited. It should be noted that the resonances due to the receiver modes occur at different frequencies in the two control cases, and this can be explained in terms of the modal behaviour of the receiving plate. The velocity cancellation control strategy constrains the out-of-plane vibration at the two junctions where the mounts are connected to the plate. Thus, for the velocity cancellation control strategy, the plate can be assumed to be simply supported at the four edges and pinned at the two junction points. This new configuration of the boundary conditions increases the stiffness of the plate and therefore the natural frequencies occur at higher frequencies than in the reference case. On the other hand, the force cancellation control strategy does not produce any change in the displacement boundary conditions of the plate and the natural frequencies remain those of the simply supported plate. At frequencies above 200 Hz, the results obtained by the velocity and force control strategies are similar to those produced by the total power control strategy.

The control of axial power produces results which are worse than those produced by force or velocity cancellation, giving average reductions of only about 10 dB, as shown in Figure 10. Power circulation is found to be very strong in this case, which causes a lot of problems, particularly when the rigid body modes are excited after control. In fact, when the rigid body modes are excited the power transmission to the receiver plate is greater after control than before. For frequencies above 200 Hz, the control performance is similar to velocity or force cancellation. The cancellation of out-of-plane velocity or force produces poor results when the modes of the receiver are excited. The fact that these modes occur at different frequencies, as described above, suggest that using a cost function which minimizes a combination of both out-of-plane velocities and out-of-plane forces at the receiver junctions should give better control.

Also shown in Figure 10 are the results of minimizing the cost function given by the weighted sum of the squared velocity and squared force, as described in section 2. This performs very well when compared with conventional velocity or force cancellation: the rigid body modes after control are quite successfully controlled. In the frequency range between 20 and 200 Hz most of the peaks due to either velocity or force cancellation are

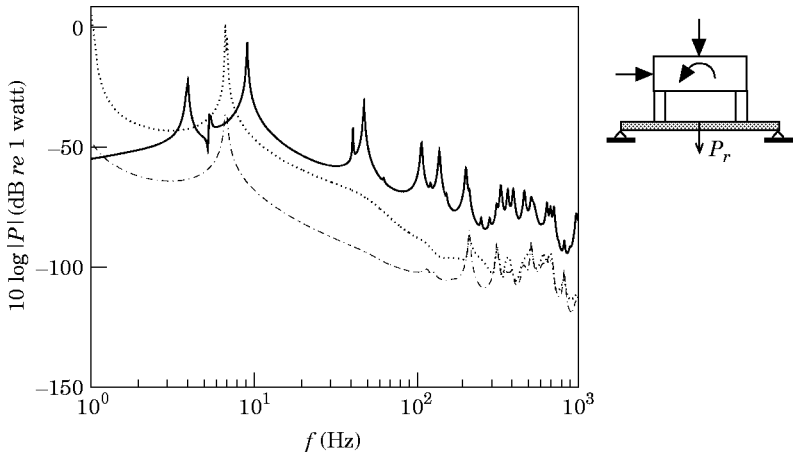

Figure 10. The power transmitted to a finite 5 mm thick plate when a combined excitation acts on the source. ——, Uncontrolled system; -·-·-, velocity and force minimization; ....., axial power minimization.

suppressed and even at higher frequencies the isolation is increased. The value of this control strategy becomes even more evident when compared with the total power minimization control strategy (see Figure 8). In general, one observes that the minimization of the weighted sum of squared values of velocities and forces gives almost as good a performance as minimizing total power except that the control of forces and velocities give slightly higher peak values (by a few decibels) at the controlled resonance frequencies.

In Figure 11 is shown the kinetic energy of the receiver plate before control and when either axial power or velocity and force are minimized. Upon comparing this plot with Figure 10, it is evident that the frequency distribution of the kinetic energy of the receiver plate before and after control is similar to the frequency distribution of power transmitted to the receiver before and after control respectively. Therefore, the power transmitted to the receiver can be considered to be a parameter which indicates the energy of the receiver structure available for causing radiated sound [4, 32].

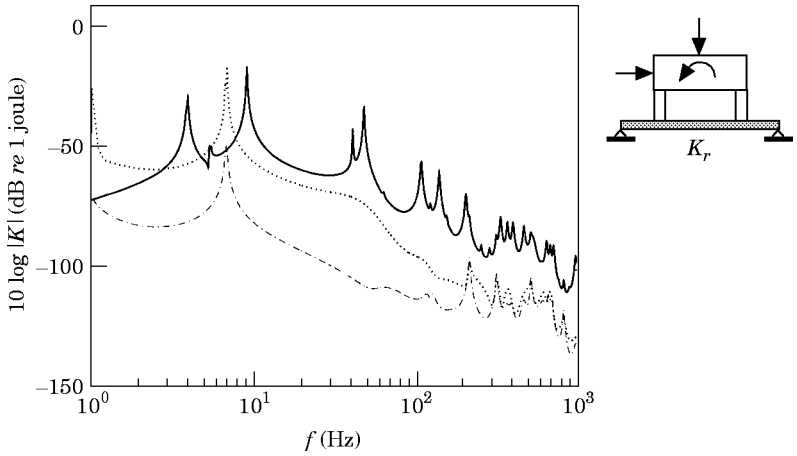

Figure 11. The total kinetic energy of the finite 5 mm thick plate when a combined excitation acts on the source. ——, Uncontrolled system; -·-·-, velocity and force minimization; ....., axial power minimization.

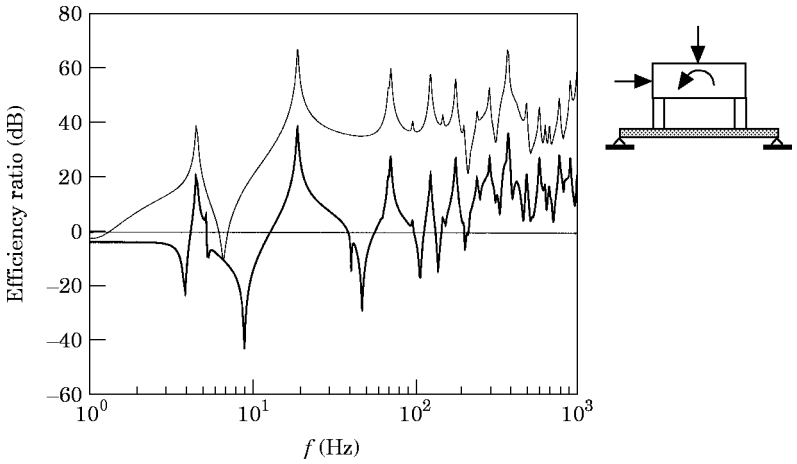

Figure 12. The efficiency of the passive isolation (——) and active isolation when velocity and force cost function is minimized (——) for a finite 5 mm thick plate.

For the isolating system with a finite plate receiver, the frequency distribution of the efficiency ratio is shown in Figure 12 before active control and for velocity and force minimization, which shows that an average efficiency improvement of about 20 dB is achieved. The active isolation is also effective at frequencies below 100 Hz where the passive isolation can produce efficiencies smaller than 1 at the receiver resonances [4].

4. ACTIVE CONTROL EFFECTIVENESS WHEN THE MOUNTS ARE INCLINED

In many applications the mounts are not vertically oriented, since by inclining them it is possible to uncouple one degree of freedom from another and achieve better passive vibration isolation [6]. In this section the effects produced by a system with inclined active mounts applied on a simply supported finite plate are examined. The inclination of the suspension is assumed to be 30°, and their geometry and physical characteristics are the same as those assumed in the previous section. The source is again excited by a combined primary excitation.

In Figure 13 is shown the power transmission when total power is controlled, while in Figures 14 and 15 are shown, respectively, the power transmitted to the receiver when velocity (out-of-plane receiver velocities) or force (out-of-plane receiver forces) are cancelled and the power transmitted to the receiver when axial power (power due to out-of-plane receiver velocities and forces) or force and velocity (sum of squared out-of-plane receiver velocities and weighted squared out-of-plane receiver forces) are minimized.

Without control, the inclined mounts react with different stiffness and with different damping values to each rigid body mode than when vertically oriented. As a consequence, different natural frequencies and oscillation amplitudes are achieved for the rigid body modes of the isolator. The natural frequencies of the transverse, axial and pitching modes are, respectively, about 4 Hz, about 5·3 Hz and about 8 Hz. The advantage of using an inclined suspension for passive isolation is evident by comparing the frequency distribution of the power transmitted to the receiver without control in Figure 8 with that shown in Figure 13. The response of the rigid body modes is slightly smaller in the second case, and better results can be achieved by finding the optimal inclination that uncouples the three-degree-of-freedom characteristics of this system.

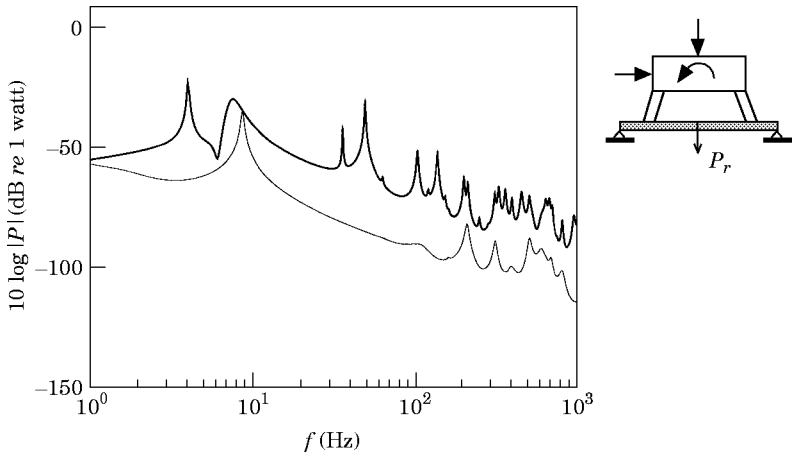

Figure 13. The power transmitted to a finite 5 mm thick plate when a combined excitation acts on the source and the mounts are 30° inclined. ——, Uncontrolled system; ———, total power minimization.

Inclining the mounts does not, however, improve the performance of the system when active control is applied. By comparing the power transmitted after control in Figures 8 and 13, it can be seen that the transmitted power after control is worse for the active isolation system with inclined mounts. The reason for this is that now the control source acts simultaneously on two degrees of freedom of the receiver (in-plane and out-of-plane directions) and so the benefit that can be produced for one degree of freedom is balanced by the vibrations generated on the other degree of freedom that is excited. The only way to avoid this problem is to use a pair of actuators in each mount, acting independently on the two degrees of freedom instead of the single actuator.

In Figures 14 and 15 are shown the results obtained when the four alternative control strategies are considered with the inclined mounts. The limitations peculiar to these approaches, presented in the previous sections, also characterize the response of the system with inclined mounts, and generate a slight worsening of the isolation.

These results suggest that active isolation when using inclined mounts performs more poorly than active isolation when using vertical mounts. Several simulations were carried

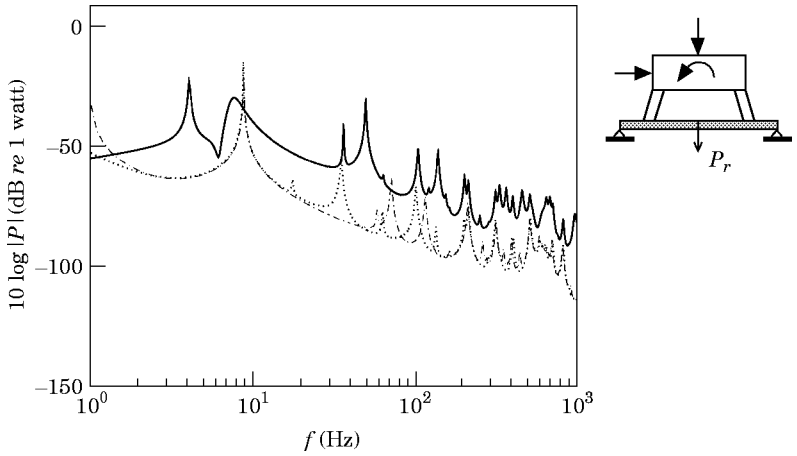

Figure 14. The Power transmitted to a finite 5 mm thick plate when a combined excitation acts on the source and the mounts are 30° inclined. ——, Uncontrolled system; -·-·-, velocity cancellation; ....., force cancellation.

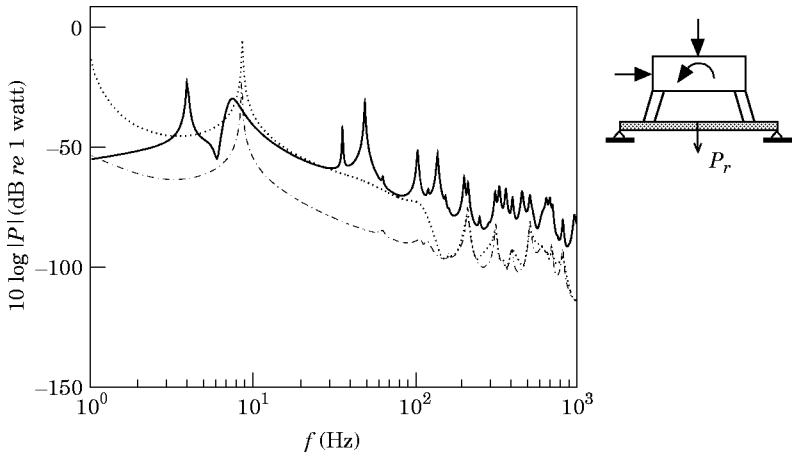

Figure 15. The Power transmitted to a finite 5 mm thick plate when a combined excitation acts on the source and the mount are 30° inclined. ——, Uncontrolled system; -·-·-, velocity and force minimization; ....., axial power minimization.

out for different inclinations of the mounts [33] and the results obtained have shown that the efficiency is worse than for vertical mounts in all cases. It can thus be concluded that the best result with an active mount when using only an axial actuator is achieved by using vertical mounts.

5. EFFECTS GENERATED BY AN UNCONTROLLED FLANKING SOURCE

In many cases, the receiver is influenced by the flanking excitations as well as by forces directly transmitted from the source through the mounts. Typically, flanking excitation can be modelled as point forces [24] or by distributed excitation due to incident noise [30]. The presence of an uncontrolled source acting at the receiver can affect the behaviour of the active control system. Scheuren *et al*. [24] produced some experimental results on the effect of a flanking source.

In this section we consider the effect of a flanking excitation consisting of an out-of-plane force (F_{zf}) acting on the simply supported receiver plate of the isolator system of Figure 1 at $x_f = 0{\cdot}5$ m and $y_f = 0{\cdot}2$ m. The total power input into the receiver (P_r) and the power supplied by the isolator (P_t) and the flanking source (P_f) are shown in Figure 16. It is important to point out that these two components of power input into the receiver are both evaluated with both the primary and flanking excitations acting together, and the interaction between these two sources affects the power transmitted by them both. The flanking excitation is considered to be an harmonic excitation, the amplitude of which has been adjusted so that the power delivered to the receiver by the flanking path action is around 15 dB less than the power transmitted by the source, as shown in Figure 16. The power input by the flanking path before control is so low in comparison to the power input by the source that it can be neglected, and the total power input into the receiver can be assumed equal to the power input by the source (in Figure 16 the thick line representing the total power input into the plate (P_r) is coincident with the thin line representing the power transmitted to the plate (P_t) by the source). The dynamics of the receiver plate before control is thus not significantly influenced by the flanking excitation, and the vibration of the plate is the same as in the case in which only the source is exciting the receiver.

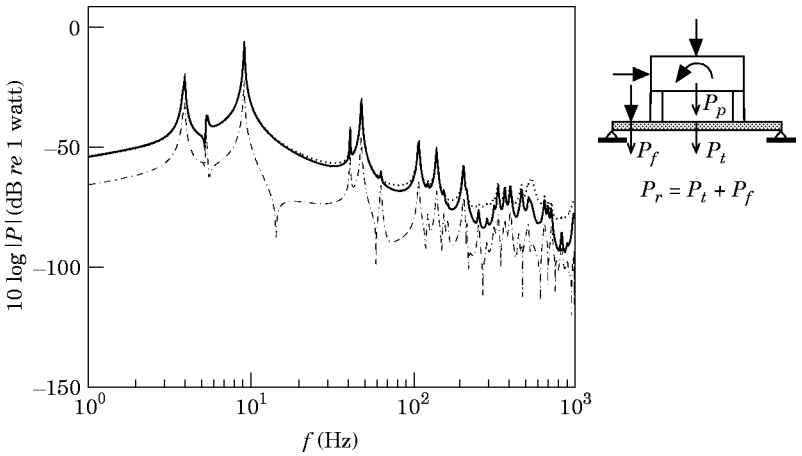

Figure 16. The power transmitted to an infinite 5 mm thick plate when a combined excitation acts on the source and a flanking excitation acts on the receiver. ——, Total power; ———, power transmitted through the mounts (coincident with (——), ..., power input to the source; -·-·-, power transmitted by the flanking path.

In Figure 17 is shown the total power input into the receiver when the total power transmitted by the isolator to the receiver is controlled. In this case, the control action is very poor and on average little attenuation is achieved. When active control is implemented at low frequency, the total power input to the receiver is actually increased. This result clearly indicates that the control source strongly interacts with the flanking source in this case. It has been found that in this case the cost function used by the control system, equation (5), can assume negative values and, since the optimal control attempts to minimize this cost function [25, 26], the control source maximizes the power absorption from the receiver instead of minimizing the power transmission to it (see also Appendix A).

Therefore, although a "weak flanking excitation" does not transmit a significant quantity of power to the receiver before control, it can cause the strategy of actively controlling the total power transmitted through the isolators to fail, since the control forces

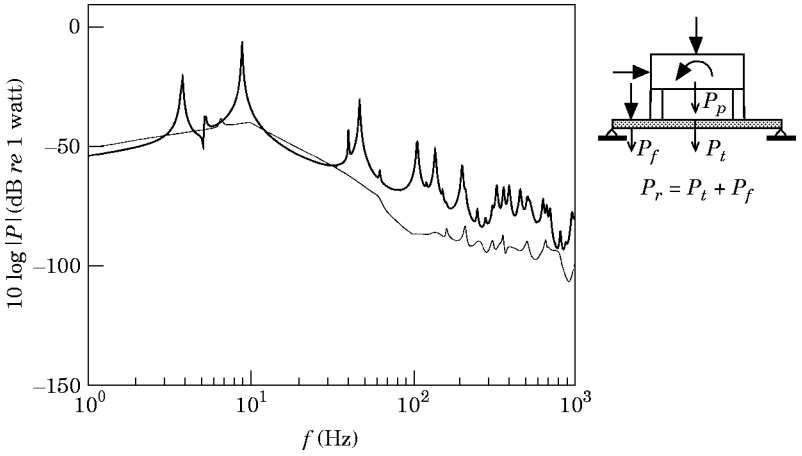

Figure 17. The power transmitted to a finite 5 mm thick plate when a combined excitation acts on the source and a flanking excitation acts on the receiver. ——, Uncontrolled system; ———, total power minimization at the mounts junctions.

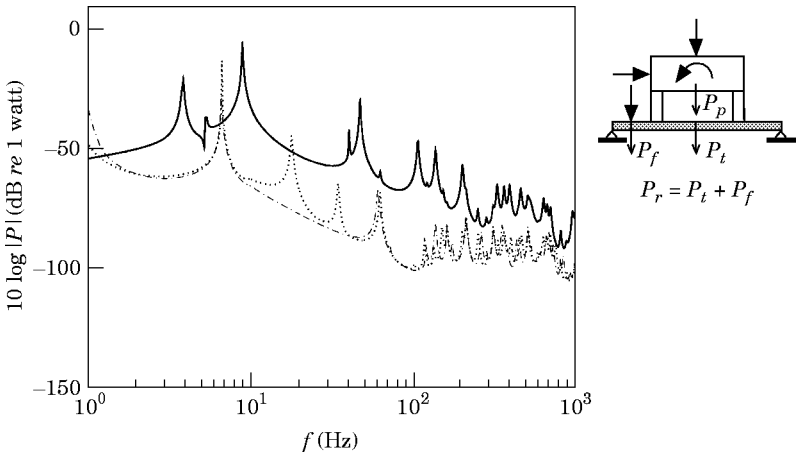

Figure 18. The power transmitted to a finite 5 mm thick plate when a combined excitation acts on the source and a flanking excitation acts on the receiver. ——, Uncontrolled system; -·-·-, velocity cancellation; ....., force cancellation.

can absorb power from the flanking path and thus increase the vibration of the receiver instead of reducing it.

In Figure 18 is shown the effects of the velocity and force control strategies, and it can be seen that these are not greatly affected by the flanking source and produce similar attenuation to that seen in Figure 9 for the system where only the source excites the receiver. This is because after control the structure is constrained from moving at the isolator mounting points, and since the flanking is close to these points, the velocities at the point of excitation of the flanking path are reduced and hence its transmitted power is also reduced.

The total power transmission when using the two alternative control approaches is shown in Figure 19. When the axial power is controlled, a similar phenomenon is observed to that which occurs with power minimization isolation. These power circulation effects are even stronger in this case, however, and very poor active isolation is achieved. The

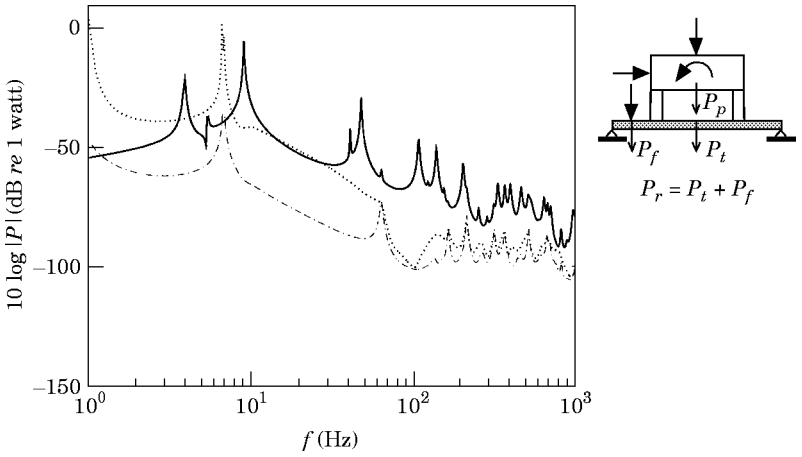

Figure 19. The power transmitted to a finite 5 mm thick plate when a combined excitation acts on the source and a flanking excitation acts on the receiver. ——, Uncontrolled system; -·-·-, velocity and force minimization; ....., axial power minimization.

control of velocities and forces, equation (19), on the other hand, produces good results. Comparing Figures 10 and 19 shows that the presence of the flanking source does have some effect on the control action, but this is quite weak. Thus the main conclusion is that using velocity and force control is still better than using either velocity or force cancellation.

When a system is excited by several sources and it is not possible to measure the total power input into the system from all of them, it is thus preferable to use the traditional control approaches of velocity or force cancellation, rather than any power based strategy, although the best results are obtained by using the simultaneous control of velocity and force.

6. EFFECTS DUE TO MEASUREMENT ERRORS

The performance of a control strategy is also influenced by errors introduced in the measurement system for the forces and velocities. These include *cross-sensitivity* and *phase matching* measurement errors.

All four control strategies studied in this paper use the measured axial velocity and axial force beneath the mounts. In the companion paper [4] it has been demonstrated that the power transmission due to the transverse and angular vibration at the receiver junctions is at least one order of magnitude smaller than that due to axial vibration. Therefore, in the following analysis, the cross-sensitivity phenomenon has been neglected and only the phase matching error has been taken into account. The measured axial velocity or axial force at the two receiver junctions has been assumed to be equal to

$$\hat{\dot{w}} = \dot{w}_r \, \mathrm{e}^{\phi_w}, \qquad \hat{N}_{zr} = N_{zr} \, \mathrm{e}^{\phi_{Nz}}, \tag{19, 20}$$

where ϕ has been assumed to have a uniform random distribution within a range of $\pm 0{\cdot}2^\circ$. These errors do not affect the velocity or force control strategies, since these two approaches use only the modulus of the velocity and force. The control strategy based on axial power minimization, however, does not involve cancellation but minimizes the product of the velocities and forces. The effect produced by corrupted measurements in the computation of power can be analyzed by considering the axial power (power due to out-of-plane velocities and forces) which, without measurement errors, is equal to

$$P = \tfrac{1}{2}\mathrm{Re}\,(N_{zr}^{*}\dot{w}_r). \tag{21}$$

This can be considered as the real component of a "complex power quantity", defined as

$$W = N_{zr}^{*}\dot{w}_r = P + \mathrm{j}Q, \tag{22}$$

in which the real part P is the "*true power*" and the complex part Q is called the "*reactive power*". These two quantities can be represented in terms of the applied force and the input mobility as

$$P = \tfrac{1}{2}\,N_{zr}|^2\mathrm{Re}\,(m_{wN_z}), \qquad Q = \tfrac{1}{2}|N_{zr}|^2\mathrm{Im}(m_{wN_z}), \tag{23, 24}$$

where the mobility term is given by $m_{wN_z} = \dot{w}_r/N_{zr}$. The observed axial power $\hat{P}$ can thus be expressed as

$$\hat{P} = \tfrac{1}{2}\mathrm{Re}\,(\hat{N}_z^{*}\hat{\dot{w}}) \tag{25}$$

and so

$$\hat{P} = \tfrac{1}{2}\mathrm{Re}\,[(N_z^{*}\dot{w})(\cos\phi_z + \mathrm{j}\sin\phi_z)], \tag{26}$$

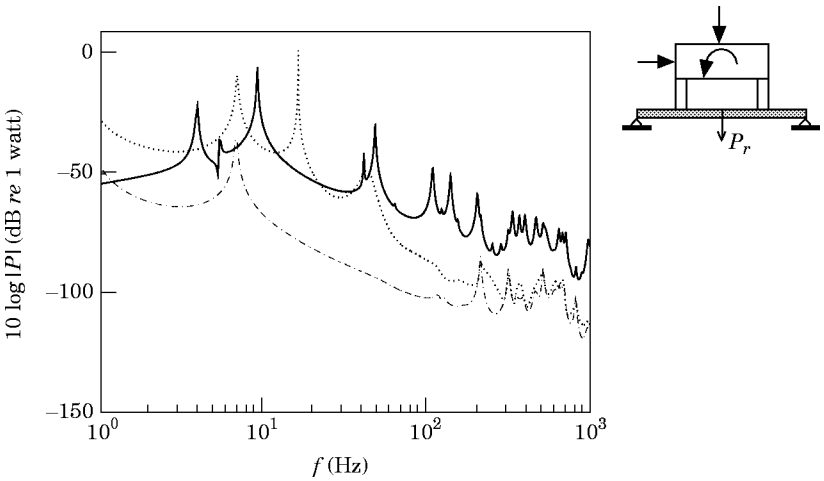

Figure 20. The power transmitted to a finite 5 mm thick plate when a combined excitation acts on the source and the control strategy is corrupted by measurement errors. ——, Uncontrolled system; -·-·-, velocity and force minimization; ....., axial power minimization.

where $\phi_z = \phi_w - \phi_{Nz}$. For small phase matching measurement errors of either $\dot{w}_r$ or N_{zr}, $\cos \phi_z \cong 1$, $\sin \phi_z \cong \phi_z$, so that

$$\hat{P} \cong \tfrac{1}{2}\mathrm{Re}[(N_z^* \dot{w})(1 + \mathrm{j}\phi_z)] = P - Q\phi_z. \tag{25}$$

This means that the measured power is corrupted by a fraction of the "reactive power" and this effect is controlled by the phase error ϕ_z. Equation (24) shows that the "reactive power" is proportional to the imaginary part of the mobility term. In the companion paper [4] it was found that the input mobility of a finite plate has a dominant imaginary component, while the input mobility of an infinite plate has a dominant real part. The measurement errors are thus expected to be more important when the plate is finite rather than when it is infinite.

In Figure 20 is shown the frequency distribution of the power transmitted to the finite receiver plate when the observed axial power and velocity and force are minimized with residual phase errors of less than $0{\cdot}2^\circ$ in the transducers. Upon comparing this picture with Figure 10, it is evident that the measurement errors greatly affect the control action when axial power is minimized. The large reactive power at the finite receiver plate combined with the circulation of power phenomenon described in section 3.1 greatly limits the effectiveness of the axial power control strategy. The control strategy of velocity and force minimization is shown to be unaffected by the presence of the phase errors, since only the modulus of the velocity and force are used.

7. FEASIBILITY OF CONTROLLER SYSTEM

The results presented in the previous sections define the physical limitations of each control strategy when using an ideal feedforward control system. In practice, a feedforward control system generally uses an internal model of the response of the system under control, the "plant", and its performance depends on the accuracy of such a model [34]. In the frequency domain the "plant response" is the complex ratio of the output of the error sensor to the input to the control actuator. Feedback controllers also often use an explicit or implicit internal model of the plant response and errors in this plant model can lead to instability [35]. The complexity of the plant response in this case is thus of

considerable importance and could be of two forms depending on whether the velocity or force signal is used in the cost function.

In this section an examination is presented on the form of these two plant responses which, at a single frequency, are given by square matrices, the elements of which are the transfer responses from the two control forces (F_{s1}, F_{s2}) to either the two velocities ($\dot{w}_{r1}$, $\dot{w}_{r2}$) or the two forces (N_{zr1}, N_{zr2}). Because the geometry of the complete isolator system considered in this paper is symmetric, the velocity or force plant matrices are also symmetric and can be written as

$$\mathbf{G}_v(\omega) = \begin{bmatrix} G_{v1}(\omega) & G_{v2}(\omega) \\ G_{v2}(\omega) & G_{v1}(\omega) \end{bmatrix}, \qquad \mathbf{G}_f(\omega) = \begin{bmatrix} G_{f1}(\omega) & G_{f2}(\omega) \\ G_{f2}(\omega) & G_{f1}(\omega) \end{bmatrix}. \tag{26}$$

where

$$G_{v1} = \dot{w}_{r1}/F_{s1} = \dot{w}_{r2}/F_{s2}, \qquad G_{v2} = \dot{w}_{r1}/F_{s2} = \dot{w}_{r2}/F_{s1},$$
$$G_{f1} = N_{zr1}/F_{s1} = N_{zr2}/F_{s2}, \qquad G_{f2} = N_{zr1}/F_{s2} = N_{zr2}/F_{s1}. \tag{27–30}$$

In Figures 21 and 22 are shown the modulus and phase of the frequency responses relating the out-of-plane velocities $\dot{w}_{r1}$ and $\dot{w}_{r2}$ to a unit axial control force $F_{s1}(G_{v1}, G_{v2})$, while in Figures 23 and 24 are shown the modulus and phase of the frequency responses relating the out-of-plane forces N_{zr1} and N_{zr2} to a unit axial control force $F_{s1}(G_{f1}, G_{f2})$. From these four figures it can be seen that when controlling the force, the diagonal plant response, G_{f1}, tends to be a relatively smooth function for frequencies above about 100 Hz (Figure 23), while the diagonal plant responses for velocity control, G_{v1} (Figure 21), are not so smooth.

Thus, if a single mount isolator system is considered, as reported in reference [3], it should be easier to implement the controller for force cancellation since, at frequencies above 100 Hz, the plant can be accurately approximated by a uniform gain. If the response of the receiving structure changes due, for example, to temperature or loading variations, all of the resonance frequencies will shift, but the higher resonances will tend to be affected to a great extent. If a fixed plant model is used, then a control strategy using only force

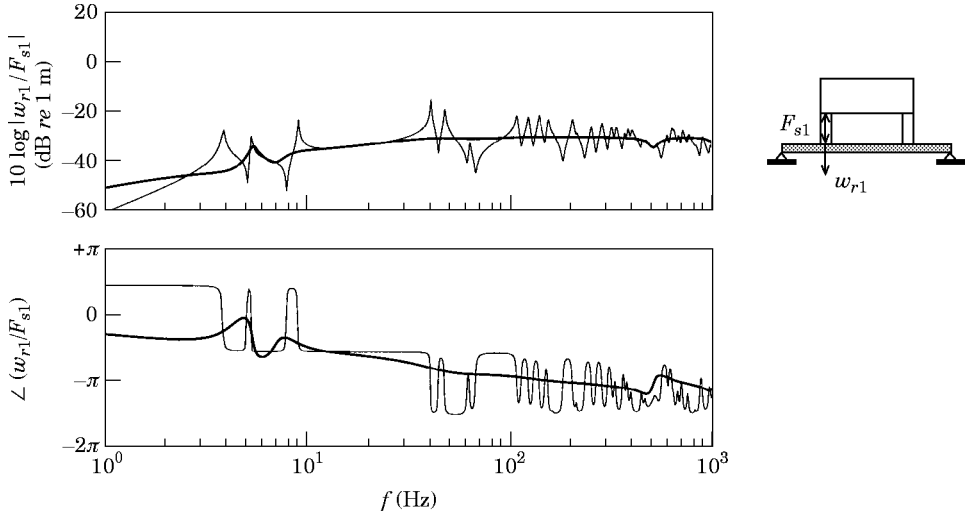

Figure 21. The modulus and phase of $\dot{w}_{r1}$, the out-of-plane velocity at receiver junction, when only unit control force $F_{s1} = 1$ is acting. ———, Finite plate; ——, infinite plate.

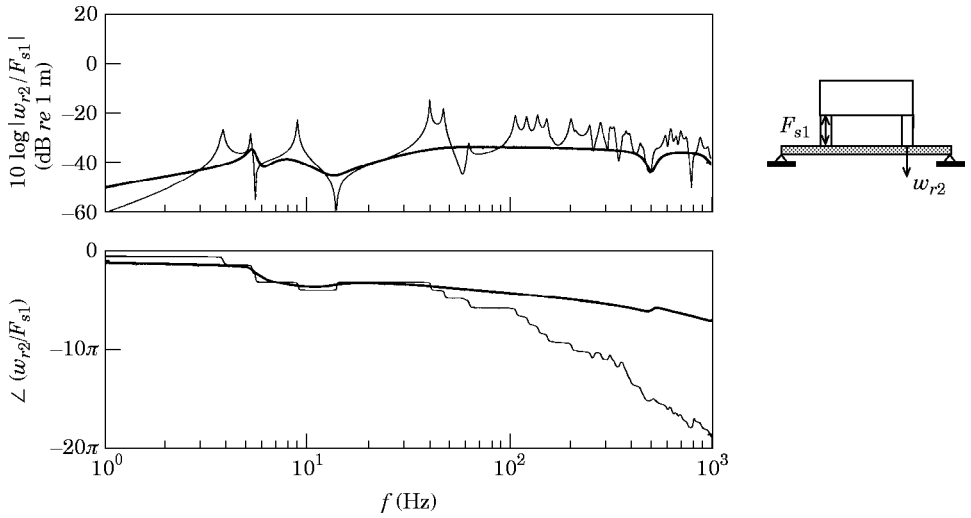

Figure 22. The modulus and phase of $\dot{w}_{r2}$, the out-of-plane velocity at receiver, when only unit control force $F_{s1} = 1$ is acting. ———, Finite plate; infinite plate; ——, infinite plate.

transducers will thus be more robust to these changes than one using velocity transducers. These observations are consistent with those of Blackwood and von Flotow [3].

However, when a two-mount isolating system is used, it may be necessary to consider both the diagonal and off-diagonal terms in the plant matrix. The off-diagonal component of the plant response for force control is shown in Figure 24, and is just as influenced by the receiver dynamics as the off-diagonal component for velocity cancellation, shown by Figure 22. Multi-channel control systems using force transducers may thus not show the same robustness to plant variations as observed for single channel systems.

When the receiving structure is more heavily damped, the resonances in the receiving structure will have less effect on both plant responses, and the extreme case of this is shown by the thick lines in Figures 21–24, in which case an infinite receiving structure has been

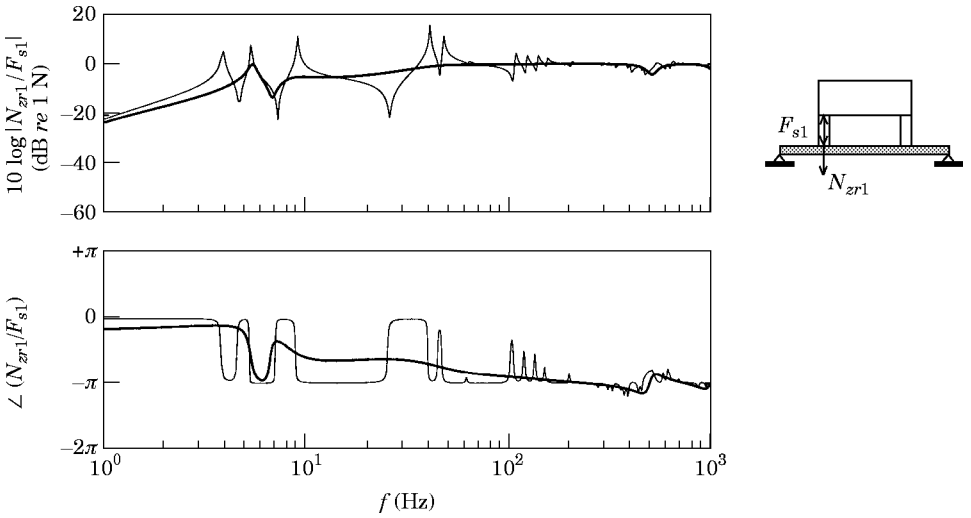

Figure 23. The modulus and phase of N_{zr1}, the out-of-plane force at receiver junction, when only unit control force $F_{s1} = 1$ is acting. ———, Finite plate; ——, infinite plate.

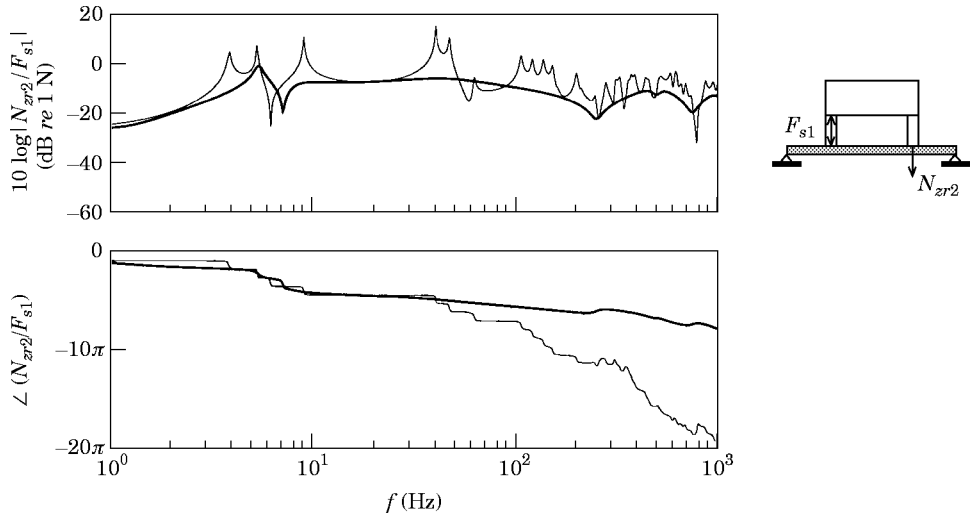

Figure 24. The modulus and phase of N_{zr2}, out-of-plane force at receiver junction, when only unit control force $F_{s1} = 1$ is acting. ———, Finite plate; ——, infinite plate.

assumed. In this case the plant responses are similarly smooth whether controlling force or velocities.

8. CONCLUSIONS

This paper presents the results of a study of active isolation from a rigid source structure through multiple mounts to a reactive receiver structure.

A detailed theoretical analysis has been presented of an active isolator modelled by using multiple-distributed mounts and a distributed receiver. In particular, a case has been studied in which the source is a rigid mass, free to move in two directions and rotate in a plane, connected to an infinite or finite plate by a pair of active mounts. These two types of receiving plate were chosen to simulate either a system with a very damped receiving structure, in which the dynamics are due only to wave propagation, or a system with a lightly damped receiver, in which the dynamics are dominated by modal behaviour. The active mounts were modelled as a ring of rubber through which the secondary force acted. At low frequencies, below 20 Hz, such an isolating system is characterized by rigid body modes, that is: a transverse mode, an axial mode and a pitching mode. At higher frequencies the response is characterised by the modes of the distributed mounts and by the modes of the receiver when it is assumed to be a finite plate.

In the analysis a matrix model is used based on input and transfer mobility or impedance terms of the three members, and the details of such a model were presented in a companion paper [4]. The vibration transmitted to the receiver has been described in terms of total structural power, since this single quantity provides a convenient way of comparing the effects of different forms of motion.

The effectiveness of minimizing the total power transmitted to the receiver has been compared with the cancellation of axial velocity or force at the receiver junctions, with the minimization of axial power and finally with the minimization of the weighted sum of square value of both the axial velocities and forces at the receiver junctions. The minimization of total power transmitted from the source to the receiver is the optimal control strategy and is used as a benchmark against which the other four strategies are

gauged. The simulations have shown an average reduction of the power transmitted to the receiver of 30 dB for both infinite and finite plates. The cancellation of velocities or forces is less effective, and on average the transmission of power to the receiver is reduced to 20 dB, but when the rigid body modes of the source are excited the power transmitted after control can be even greater than the power transmitted by the passive isolator. The simulations carried out have revealed the interesting phenomenon that after control only two rigid body modes exists. This is because the axial control forces completely decouple the axial oscillation of the source from the mounts and thus cause the axial mode to disappear. Also, because the axial vibration is now decoupled, the transverse and pitching modes are controlled only by the bending stiffness of the mounts (instead of bending and normal stiffness) and therefore their natural frequencies are reduced.

The control strategy of minimizing axial power also generally gives poor results compared with minimizing total power. The average reduction is much lower than for the case of total power minimization or velocity or force cancellation. Over a certain frequency range the power transmitted after control is even greater than the power transmitted by the passive isolator. It has been found that when the axial power is minimized the phenomenon of power circulation can occur. The cost function in this case can assume negative values indicating a process of maximization of the power absorption. The control sources tend to absorb power from the receiver through axial vibration and this power is supplied to the plate by the transverse and angular vibration of the mounts. Hence the transmission of power to the receiver after control can be a complex phenomenon that requires a sophisticated multi-degree-of-freedom model to be accurately represented.

Finally, the minimization of a cost function which consists of the weighted sum of squares of the axial velocity and force has been shown to provide a particularly interesting result, since the isolation is then very close to the one achieved when total power is controlled. This approach has been found to be particularly effective when the receiver is a finite system. The reason for this is related to the dynamics of the receiver system after control. When velocity or force cancellation control strategies are used, poor results are achieved when the modes of the receiver system are excited. These modes occur at different frequencies in the two control cases, and therefore the problem generated by the resonances of the receiver system can be avoided by using a control strategy in which velocity and force are simultaneously minimized.

In the second part of the paper the presence of an uncontrolled flanking source has been considered, the amplitude of which has been adjusted so that the power delivered to the receiver by the flanking path is around 15 dB less than the power transmitted to the receiver through the mounts. Therefore the dynamics of the receiver plate before control are not significantly influenced by the flanking excitation, and the vibration of the plate is similar to that in the case in which the mounts are the only source of transmission to the receiver. The simulations carried out have shown that this flanking excitation can adversely affect the two control strategies involving power minimization. The problem is due to the fact that the control sources can maximize power absorption by the secondary source instead of minimizing the total power transmitted from the source to the receiver. This power is supplied by the flanking source, and although it is negligible before control it can become a significant source of power when it interacts with the control forces. The strategy of minimizing the total observed power thus can only be considered as being optimal if the power produced by all of the sources acting on the receiver and related to all degrees of freedom of the system are accounted for in the measurement.

In the third part of the paper the effects generated by errors in measuring the controlled parameters has been considered. The control strategies of cancellation of velocity, force and the minimization of velocity and force are all robust to measurement errors, while the

power control functions are sensitive to small measurement errors which make these approaches very demanding in terms of sensor technology when compared with the control strategies of cancelling forces or velocities.

Finally, the demands that the various control strategies place on the control system have been briefly considered. Of particular interest was the potential change in the various plant responses due to changes in receiver dynamics, which could affect the robustness of a control system. It has been found that, when a single mount isolating system is used, the force cancellation strategy leads to a plant response that is less affected by the receiver dynamics than the strategy of velocity cancellation. However, when the isolator system has multiple mounts the advantages of force cancellation are not as clear-cut, since the plant cross coupling terms for both velocity and force control appear to be similarly offended by the receiver dynamics.

ACKNOWLEDGMENTS

The content of this paper is part of a Brite-Euram project supported by the EC under the contract BREU 7228 ASPEN, "Active Control of Structured Vibration Using Power Transmission Methods".

REFERENCES

1. D. Karnopp 1995 *Transaction of the American Society of Mechanical Engineers* **177**, 177–185. Active and semi-active vibration isolation.
2. A. M. Beard, A. H. von Flotow and D. W. Schubert 1994 *Proceedings of the IUTAM Symposium on the Active Control of Vibrations*, *Bath U.K.*, 101–108. A practical product implementation of an active/passive vibration isolation system.
3. G. H. Blackwood and A. H. von Flotow 1993 *Proceedings of the Conference on Recent Advances in Active Control of Sound and Vibration*, *VPI Blacksburg Virginia*, 482–494. Active control for vibration isolation despite resonant structural dynamics: a trade study of sensors, actuators and configurations.
4. P. Gardonio, S. J. Elliott and R. J. Pinnington 1997 *Journal of Sound and Vibration* **207**, 61–93. Active isolation of structural vibrations on a multiple-degree-of-freedom system, part I: dynamics of the system.
5. W. T. Thomson 1993 *Theory of Vibration With Applications* (fourth edition). Englewood Cliffs, New Jersey: Prentice-Hall.
6. C. M. Harris 1961 *Shock and Vibration Handbook*. New York: McGraw-Hill.
7. R. G. White and J. G. Walker (editors) 1982 *Noise and Vibration*. Chichester: Ellis Horwood.
8. S. Lefebvre, C. Guigou and C. R. Fuller 1992 *Journal of Sound and Vibration* **155**, 185–188. Experiments on active isolation using distributed PVDF error sensors.
9. C. Guigou and C. R. Fuller 1994 *Journal of the Acoustical Society of America* **96**(1), 294–299. Active isolation of vibration with adaptive structures.
10. A.H. von Flotow 1988 *Proceedings of the 27th Conference on Decision and Control*, *Austin*, *Texas*, 2029–2033. An expository overview of active control of machinery mounts.
11. M. D. Jenkins, P. A. Nelson, R. J. Pinnington and S. J. Elliott 1991 *Journal of Sound and Vibration* **166**, 117–140. Active isolation of periodic machinery vibrations.
12. K. B. Scribner, L. A. Sievers and A. H. von Flotow 1993 *Journal of Sound and Vibration* **167**, 17–40. Active narrow-band vibration isolation of machinery noise from resonant substructures.
13. J. Pan, J. Pan and C. H. Hansen 1992 *Journal of the Acoustical Society of America* **92**(2), 895–907. Total power flow from a vibrating rigid body to a thin panel through multiple elastic mounts.
14. R. J. Pinnington and R. G. White 1980 *Journal of Sound and Vibration* **75**, 179–197. Power flow through machine isolators to resonant and non-resonant beams.
15. R. J. Pinnington 1987 *Journal of Sound and Vibration* **118**, 515–530. Vibrational power transmission to a seating of a vibration isolated motor.

16. D. W. Miller, S. R. Hall and A. H. von Flotow 1990 *Journal of Sound and Vibration* **140**, 475–497. Optimal control of power flow at structural junctions.
17. J. Pan and C. H. Hansen 1993 *Journal of the Acoustical Society of America* **89**(1), 200–209. Active control of total vibratory power flow in a beam, I: physical system analysis.
18. Y. K. Koh and R. G. White 1996 *Journal of Sound and Vibration* **196**, 495–508. Analysis and control of vibrational power transmission to machinery supporting structures subjected to a multi-excitation system, part II: vibrational power analysis and control scheme.
19. G. P. Gibbs and C. R. Fuller 1992. *American Institute of Aeronautics and Astronautics Journal* **30**(2), 457–463. Experiments on active control of vibrational power flow using piezoceramic actuators/sensors.
20. M. J. Brennan, S. J. Elliott and R. J. Pinnington 1995 *Journal of Sound and Vibration* **186**, 657–688. Strategies for the active control of flexural vibration on a beam.
21. M. Nam, S. I. Hayek and S. D. Sommerfeldt 1995 *Proceedings of the Conference Active* **95**, *Newport Beach*, *California*, 209–220. Active control of structural intensity in connected structure.
22. J. Pan and C. H. Hansen 1993 *Journal of the Acoustical Society of America* **93**(4), 1947–1953. Active control of power flow from a vibrating rigid body to a flexible panel through two active isolators.
23. J. Pan, C. H. Hansen and J. Pan 1993 *Journal of the Acoustical Society of America* **94**(3), 1425–1434. Active isolation of a vibration source from a thin beam using a single active mount.
24. J. Scheuren, W. Bohm, M. Dorle, J. Winkler and W. Zoller 1995 *Proceedings of the Conference Active* **95**, *Newport Beach*, *California*, 79–88. Experiments with active vibration isolation.
25. P. A. Nelson and S. J. Elliott 1992 *Active Control of sound*. London: Academic Press. 1991.
26. C. R. Fuller, S. J. Elliott and P. A. Nelson 1996 *Active Control of Vibration*. London: Academic Press.
27. G. Pavic 1995 *Proceedings of ACTIVE* 95, *Newport Beach*, *California*, 197–208. Comparison of different strategies of active vibration control.
28. P. A. Nelson, M. D. Jenkins and S. J. Elliott 1987 *Proceedings of Noise Control* '87, 425–430. Active isolation of periodic vibrations.
29. J. I. Soliman and M. G. Hallam 1968 *Journal of Sound and Vibration* **8**, 329–351. Vibration isolation between non-rigid machines and non-rigid foundations.
30. R. J. Pinnington 1987 *Journal of Sound and Vibration* **118**, 515–530. Vibrational power transmission to a seating of a vibration isolated motor.
31. O. Bardou, P. Gardonio, S. J. Elliott and R. J. Pinnington 1996 *Journal of Sound and Vibration*. Active power minimization and power absorption in a plate with force and moment excitation.
32. A. Moorhouse and B. B. Gibbs 1995 *Acoustic Bulletin*, *November/December*, 21–26. Structure-borne sound—the unheard acoustic.
33. P. Gardonio, S. J. Elliott and R. J. Pinnington 1995 *ISVR Technical Report No*. 65, *University of Southampton*. Active isolation of multiple-degree-of-freedom vibrations transmission between a source and a receiver.
34. S. J. Elliott, C. C. Boucher and P. A. Nelson 1992 *IEEE Transaction*s ASSP-40, 1041–1052. The behaviour of a multiple channel active control system.
35. S. J. Elliott and T. J. Sutton 1996 *IEEE Transactions on Speech and Audio Processing*. Performance of feedforward and feedback systems for active control.
36. S. Laugesen, 1994 *Proceedings of the IUTAM Symposium on the Active Control of Vibrations*, *Bath*, 241–246. An example of power based active control of vibrations.

APPENDIX A: POWER MINIMIZATION WITH UNOBSERVED PRIMARY EXCITATION

In this Appendix an examination is presented of the theoretical behaviour of the power minimization strategy if not all the primary excitations acting on the system are observed in the cost function being minimized. The unobserved primary excitation may be a separate flanking path, or it may be a component of the primary source motion, the influence of which is not observed by the sensors. In general, there may also be force components of the secondary actuation which are not observed by the control system, but these are excluded here for clarity.

One thus considers three separate vectors of forces acting on the structure, which may include moments: $\mathbf{f}_p$ is the vector of primary forces measured by the control system, $\mathbf{f}_s$ is the vector of secondary forces measured by the control system and $\mathbf{f}_u$ is the vector of unobserved forces acting on the structure.

The power input to the structure, as observed by the control system, can be written as

$$P_0 = \tfrac{1}{2}\mathrm{Re}\,(\mathbf{f}_p^{\mathrm{H}}\mathbf{v}_p + \mathbf{f}_s^{\mathrm{H}}\mathbf{v}_s), \tag{A1}$$

where $\mathbf{v}_p$ and $\mathbf{v}_s$ are the vectors of velocities at the points of application of the primary and secondary forces. These velocities are generated by the primary, secondary and unobserved forces, however, and can thus be written as

$$\begin{Bmatrix}\mathbf{v}_p\\ \mathbf{v}_s\end{Bmatrix} = \begin{bmatrix}\mathbf{M}_{pp} & \mathbf{M}_{ps}\\ \mathbf{M}_{sp} & \mathbf{M}_{ss}\end{bmatrix}\begin{Bmatrix}\mathbf{f}_p\\ \mathbf{f}_s\end{Bmatrix} + \begin{bmatrix}\mathbf{M}_{pu}\\ \mathbf{M}_{su}\end{bmatrix}\mathbf{f}_u, \tag{A2}$$

where $\mathbf{M}_{pp}$, $\mathbf{M}_{ps}$, $\mathbf{M}_{sp}$, $\mathbf{M}_{ss}$, $\mathbf{M}_{pu}$ and $\mathbf{M}_{su}$ are the input and transfer mobility matrices for the various excitation points on the structure. Equation (A2) for the velocities at points of application of the primary and secondary forces can be substituted into equation (A1) to give an expression for the observed power which, when written in Hermitian quadratic form [25], becomes

$$\begin{aligned}\mathbf{P}_0 = \tfrac{1}{2}[&\mathbf{f}_s^{\mathrm{H}}\mathbf{R}_{ss}\mathbf{f}_s + \mathbf{f}_s^{\mathrm{H}}(\mathbf{R}_{sp}\mathbf{f}_p + \tfrac{1}{2}\mathbf{M}_{su}\mathbf{f}_u) + (\mathbf{f}_p^{\mathrm{H}}\mathbf{R}_{ps}^{\mathrm{H}} + \tfrac{1}{2}\mathbf{f}_u^{\mathrm{H}}\mathbf{M}_{us}^{\mathrm{H}})\mathbf{f}_s\\ &+ \mathbf{f}_p^{\mathrm{H}}\mathbf{R}_{pp}^{\mathrm{H}}\mathbf{f}_p + \mathbf{f}_p^{\mathrm{H}}\mathbf{M}_{pu}\mathbf{f}_u + \mathbf{f}_u^{\mathrm{H}}\mathbf{M}_{up}^{\mathrm{H}}\mathbf{f}_p],\end{aligned} \tag{A3}$$

where $\mathbf{R}_{pp}$, $\mathbf{R}_{ps}$, $\mathbf{R}_{sp}$ and $\mathbf{R}_{ss}$ are the matrices of the real parts of the elements of $\mathbf{M}_{pp}$, $\mathbf{M}_{ps}$, $\mathbf{M}_{sp}$, $\mathbf{M}_{ss}$. Equation (A3) has a minimum value for a set of secondary forces given by

$$\mathbf{f}_s = -\mathbf{R}_{ss}^{-1}[\mathbf{R}_{sp}\mathbf{f}_p + \tfrac{1}{2}\mathbf{M}_{su}\mathbf{f}_u]. \tag{A4}$$

It is interesting to note that this set of secondary forces is the sum of those that would have minimized the true input power if there had been no unobserved excitations ($\mathbf{f}_u = 0$) and those that maximize the power absorption of $\mathbf{f}_s$ in the presence of the unobserved excitation only ($\mathbf{f}_p = 0$).

Equation (A4) can be used to obtain an expression for the true input power to the structure after control, although this is a little unwieldy. The main point to note is that if all the sources of power input to the structure are not accounted for in the cost function being minimized, the power minimization control strategy will act to absorb power from the unobserved excitations to the system. This has previously been shown to run the risk of increasing the total power supplied to the system [31, 33, 36].